Build up of off-diagonal long-range order in microcavity exciton-polaritons across the parametric threshold

R. Spano,[1,2,*] J. Cuadra,[1] C. Lingg,[1] D. Sanvitto,[1,3] M. D. Martin,[1,4] P. R. Eastham,[5] M. van der Poel,[6] J. M. Hvam,[6] and L. Viña[1,4,7]

[1]*Dept. Física Materiales,Universidad Autónoma de Madrid, Madrid 28049, Spain*
[2]*Current address: Laboratoire d'Optoélectronique Quantique, École Polytechnique Fédérale de Lausanne (EPFL), Station 3, CH-1015 Lausanne, Switzerland*
[3]*Current address: NNL, Istituto Nanoscienze - CNR, Via Arnesano, 73100 Lecce, Italy, Istituto Italiano di Tecnologia, IIT-Lecce, Via Bersanti, 73010 Lecce, Italy*
[4]*Instituto de Ciencia de Materiales "Nicolás Cabrera", Universidad Autónoma de Madrid 28049 Madrid, Spain*
[5]*School of Physics, Trinity College, Dublin 2, Ireland*
[6]*DTU Fotonik, Tech. Univ. Denmark, Ørsteds Plads 343, DK-2800 Kgs. Lyngby, Denmark*
[7]*Instituto de Física de la Materia Condensada, Universidad Autónoma de Madrid, Madrid 28049, Spain*

[*]*rita.spano@uam.es*

Abstract: We report an experimental study of the spontaneous spatial and temporal coherence of polariton condensates generated in the optical parametric oscillator configuration, below and at the parametric threshold, and as a function of condensate area. Above the threshold we obtain very long coherence times (up to 3 ns) and a spatial coherence extending over the entire condensate (40 μm). The very long coherence time and its dependence on condensate area and pump power reflect the suppression of polariton-polariton interactions by an effect equivalent to motional narrowing.

OCIS codes: (030.1640) Coherence; (140.3945) Microcavities; (020.1475) Bose-Einstein condensates; (100.3175) Interferometric imaging; (240.5420) Polaritons; (190.4410) Nonlinear optics, parametric processes.

References and links

1. *Physics of Semiconductor Microcavities*, ed. B. Deveuad (Wiley-VCH, Berlin, 2007).
2. O. Penrose and L. Onsager, "Bose-Einstein Condensation and Liquid Helium," Phys. Rev. **104**, 576–584 (1956).
3. J. Kasprzak, M. Richard, S. Kundermann, A. Baas, P. Jeambrun, J. M. J. Keeling, F. M. Marchetti, M. H. Szymańska, R. André, J. L. Staehli, V. Savona, P. B. Littlewood, B. Deveaud, and Le Si Dang, "Bose-Einstein condensation of exciton polaritons," Nature **443**, 409–414 (2006).
4. E. Wertz, L. Ferrier, D. D. Solnyshkov, R. Johne, D. Sanvitto, A. Lemaitre, I. Sagnes, R. Grousson, A. V. Kavokin, P. Senellart, G. Malpuech, and J. Bloch, "Spontaneous formation and optical manipulation of extended polariton condensates," Nature Phys. **6**, 860–864 (2010).
5. L. Pitaevskii and S. Stringari, *Bose-Einstein condensation* (Oxford University Press, Oxford, 2003).
6. F. P. Laussy, G. Malpuech, A. Kavokin, and P. Bigenwald, "Spontaneous Coherence Buildup in a Polariton Laser," Phys. Rev. Lett. **93**, 016402 (2004).
7. K. G. Lagoudakis, B. Pietka, M. Wouters, R. André, and B. Deveaud-Plédran, "Coherent Oscillations in an Exciton-Polariton Josephson Junction," Phys. Rev. Lett. **105**, 120403 (2010).
8. A. Amo, T. C. H. Liew, C. Adrados, R. Houdré, E. Giacobino, A. V. Kavokin, and A. Bramati, "Exciton-polariton spin switches," Nat. Photonics **4**, 361–366 (2010).

#185756 - $15.00 USD Received 22 Feb 2013; revised 15 Apr 2013; accepted 17 Apr 2013; published 25 Apr 2013

9. R. M. Stevenson, V. N. Astratov, M. S. Skolnick, D. M. Whittaker, M. Emam-Ismail, A. I. Tartakovskii, P. G. Savvidis, J. J. Baumberg, and J. S. Roberts, "Continuous wave observation of massive polariton redistribution by stimulated scattering in semiconductor microcavities," Phys. Rev. Lett. **85**, 3680–3683 (2000).
10. J. J .Baumberg, P. G. Savvidis, R. M. Stevenson, A. I. Tartakovskii, M. S. Skolnick, D. M. Whittaker, and J. S. Roberts, "Parametric oscillation in a vertical microcavity: A polariton condensate or micro-optical parametric oscillation," Phys. Rev. B **62**, R16247–16250 (2000).
11. A. I. Tartakovskii, D. N. Krizhanovskii, and V. D. Kulakovskii, "Polariton-polariton scattering in semiconductor microcavities: Distinctive features and similarities to the three-dimensional case," Phys. Rev. B **62**, R13298–13301 (2000).
12. I. Carusotto and C. Ciuti, "Spontaneous microcavity-polariton coherence across the parametric threshold: Quantum Monte Carlo studies," Phys. Rev. B **72**, 125335 (2005).
13. In this work we consider two kinds of threshold, associated with tuning the pump energy and power. They are denoted E_{Th} and P_{Th} respectively.
14. D. M. Whittaker and P. R. Eastham, "Coherence properties of the microcavity polariton condensate," Europhys. Lett. **87**, 27002 (2009).
15. F. Tassone and Y. Yamamoto, "Lasing and squeezing of composite bosons in a semiconductor microcavity," Phys. Rev. A **62**, 063809 (2000).
16. D. Porras and C. Tejedor, "Linewidth of a polariton laser: Theoretical analysis of self-interaction effects," Phys. Rev. B **67**, 161310(R) (2003).
17. D. N. Krizhanovskii, D. Sanvitto, A. P. D. Love, M. S. Skolnick, D. M. Whittaker, and J. S. Roberts, "Dominant Effect of Polariton-Polariton Interactions on the Coherence of the Microcavity Optical Parametric Oscillator," Phys. Rev. Lett. **97**, 097402 (2006).
18. F. P. Laussy, I. A. Shelykh, G. Malpuech, and A. Kavokin, "Effects of Bose-Einstein condensation of exciton polaritons in microcavities on the polarization of emitted light," Phys. Rev. B **73**, 035315 (2006).
19. A. Berthelot, I. Favero, G. Cassabois, C. Voisin, C. Delalande, Ph. Roussignol, R. Ferreira, and J. M. Gérard, "Unconventional motional narrowing in the optical spectrum of a semiconductor quantum dot," Nat. Phys. **2**, 759–764 (2006).
20. D. N. Krizhanovskii, K. G. Lagoudakis, M. Wouters, B. Pietka, R. A. Bradley, K. Guda, D. M. Whittaker, M. S. Skolnick, B. Deveaud-Plédran, M. Richard, R. André, and Le Si Dang, "Coexisting nonequilibrium condensates with long-range spatial coherence in semiconductor microcavities," Phys. Rev. B **80**, 045317 (2009).
21. H. Deng, G. S. Solomon, R. Hey, K. H. Ploog, and Y. Yamamoto, "Spatial Coherence of a Polariton Condensate," Phys. Rev. Lett. **99**, 126403 (2007).
22. H. P. Baltes, "Coherence and the radiation laws," Appl. Phys. **12**, 221–244 (1977).
23. M. Richard, M. Wouters, and L. S. Dang, in *Optical Generation and Control of Quantum Coherence in Semiconductor Nanostructures*, NanoScience and Technology **146**, eds. G. Slavcheva and P. Roussignol (Springer-Verlag Berlin 2010) Chap. 11.
24. The detuning δ is defined as the difference between the bare cavity and exciton energies.
25. A. P. D. Love, D. N. Krizhanovskii, D. M. Whittaker, R. Bouchekioua, D. Sanvitto, S. Al Rizeiqi, R. Bradley, M. S. Skolnick, P. R. Eastham, R. André, and Le Si Dang, "Intrinsic Decoherence Mechanisms in the Microcavity Polariton Condensate," Phys. Rev. Lett. **101**, 067404 (2008).
26. A. Baas, J.-Ph. Karr, M. Romanelli, A. Bramati, and E. Giacobino, "Quantum Degeneracy of Microcavity Polaritons," Phys. Rev. Lett. **96**, 176401 (2006).
27. M. Wouters and I. Carusotto, "Goldstone mode of optical parametric oscillators in planar semiconductor microcavities in the strong-coupling regime," Phys. Rev. A **76**, 043807 (2007).
28. P. R. Eastham and P. B. Littlewood, "Finite-size fluctuations and photon statistics near the polariton condensation transition in a single-mode microcavity," Phys. Rev. B **73**, 085306 (2006).
29. P.R. Eastham, "Mode locking and mode competition in a nonequilibrium solid-state condensate," Phys. Rev. B **78**, 035319 (2008).

1. Introduction

Planar microcavity exciton-polaritons are composite particles generated by strong coupling between excitons and cavity photons that, below the Mott transition, follow the Bose statistics. They have been extensively investigated in the past decades for their unique properties, such as very light effective mass and the consequent high critical temperature for condensation [1]. It is well known that the occurrence of such a phase transition is accompanied by the onset of long range phase coherence [2]. In fact, since the unambiguous demonstration of polariton condensation its coherence properties have been investigated [3], and the attention of the scientific community on the matter is high, as witnessed by the recent work by Wertz *et al*. on

#185756 - $15.00 USD Received 22 Feb 2013; revised 15 Apr 2013; accepted 17 Apr 2013; published 25 Apr 2013

1D ballistically expanding condensates [4], which demonstrates an extremely large coherence. Moreover, the extension and eventually the decay of the spatial coherence can give useful information on the kind of transition the system undergoes [5,6]. Recently, polariton condensates have attracted intense attention for their potential application in the field of quantum information, and also some properties suitable for such applications, like Josephson oscillations and spin-switching, have been already demonstrated [7,8]. Therefore, the achievement of extended spatial and temporal coherence for polariton condensate is crucial.

Polariton condensates can be created using off-resonant, resonant or under parametric optical excitation. The optical parametric oscillation (OPO) is a third order non-linear phenomenon, arising from interactions between the excitonic components of the polaritons. It takes place when two pump polaritons at the inflection point of the lower polariton branch (LPB), scatter efficiently into a signal and an idler polariton [9–11]. Spatial coherence properties have been studied theoretically for the OPO condensate by Carusotto and Ciuti [12]. They investigated numerically the first-order coherence function ($g^{(1)}$) for a finite condensate paying special attention to its behaviour across the OPO parametric threshold (E_{Th}) [13]. It is found that, for excitation frequencies ω_p below that of the threshold, $g^{(1)}$ has a finite correlation length. Increasing ω_p in order to approach E_{Th}, mantaining fixed the pump angle (and therefore the wavevector), they predict the build up of macroscopic phase coherence extending over the entire condensate [12]. In this regime the spatial fluctuations are negligible, so the temporal coherence properties should be captured by the theory of Whittaker and Eastham [14]. In this theory the temporal coherence is limited by fluctuations in the particle number, which due to the polariton-polariton interactions imply a broadening of the emission [15–18]. This broadening mechanism, however, would be suppressed if the intensity fluctuations relax rapidly, in a form of motional narrowing effect [19]. Thus for appropriate pump powers and condensate areas very long coherence times could be obtained.

Using a high-quality sample and a narrow-bandwidth pump laser we obtain spatially extended single-mode polariton condensates, with uniform spatial coherence extending over our entire pump spot. The temporal coherence decay of our condensates reveals the two timescales associated with the interaction-induced broadening of the condensate and the relaxation of intensity fluctuations. We show that the finite-size scaling laws describing the variation of these timescales with condensate area qualitatively agree with theory.

The main factor that limits the coherence is the quality of the cavity: the presence of defects creates a disorder potential that traps the condensate, potentially leading to multi-mode and inhomogeneous states [20]. Another, very important, detrimental effect is caused by the fluctuations of the excitation laser that hinder the attainment of the intrinsic coherence of the condensate. Initial studies [3, 20, 21] have been performed by non-resonantly pumping the microcavity, and in such cases the resulting distribution of the population at the bottom of the lower polariton branch is subjected to fluctuations due to the reservoir of particles at the bottleneck. These fluctuations, broadening the distribution of polaritons in energy and momentum space, translate, according to the Wiener-Khinchin identity [22, 23], into a faster decay of the temporal and spatial coherence. Although analogous broadening by the fluctuating population of pump polaritons can occur in the OPO [17], the threshold pump density (P_{Th}) for a resonant-gain process is much lower than that for non-resonant gain and the effect of the reservoir polaritons is not relevant, since the reservoir is either completely empty or very weekly occupied. Thus the coherence exhibited by an OPO polariton-condensate is expected to decay over much longer times and larger distances than the one produced by non-resonant techniques. Here we realize experimentally a spatially extended, and with long temporal coherence, condensate in the OPO configuration and identify the mechanism driving the extended temporal coherence.

#185756 - $15.00 USD Received 22 Feb 2013; revised 15 Apr 2013; accepted 17 Apr 2013; published 25 Apr 2013

2. Sample and experimental setup

To avoid that the pump fluctuations conceal the genuine coherence properties of the condensate, we use a CW monomode laser with a very narrow bandwidth of 75 kHz to excite the sample, which is a high-quality λ-microcavity grown by molecular beam epitaxy, composed by 16 periods of $\lambda/4$ AlAs/$Al_{0.15}Ga_{0.85}As$ on its top and 25 periods on its bottom. A single 10-nm GaAs/$Al_{0.3}Ga_{0.7}As$ QW is placed at the antinode of the cavity. The Rabi splitting is 4.2 meV and we select a uniform area of the sample with a small defect density and a detuning of $\delta \sim -3.8$ meV [24]. In order to investigate the spatial coherence properties of a 2D condensate we create one with a diameter of $\sim 40\,\mu$m, by pumping resonantly the LPB close to its inflection point, with a Gaussian laser beam, maintaining the temperature of the sample at 10 K. We adopt the experimental conditions to drive the sample into the OPO regime at the parametric threshold, E_{Th}, and then we follow a similar approach to that in [12], i.e., we decrease the pump frequency ω_p keeping fixed the angle of incidence.

3. Results

To evaluate the coherence of the condensate the signal emission is analyzed using a Mach-Zehnder interferometer. On one of the arms of the interferometer a retro reflector mirror is mounted, which flips the image of the condensate in a centrosymmetric way. Recombining, at the output of the interferometer, the image of the condensate with its flipped image allows evaluating the coherence of each point (x,y) with respect to its opposite counterpart $(-x,-y)$. In this way we access to the first order coherence function $g^{(1)}\left[(x,y),(-x,-y)\right] = \frac{\langle E^*(x,y)E(-x,-y)\rangle}{\langle E^*(x,y)\rangle\langle E(-x,-y)\rangle}$ [2, 3]. To extract the coherence of the condensate the retroreflector mirror is moved, using a piezo translation stage, few wavelengths around the zero delay position, adding a short delay Δt to the retroreflector arm with respect to the other arm. For each measurement the intensities of the two arms were acquired and used in the following normalized expression of the interference pattern: $I_{Norm}\left[(x,y),(-x,-y)\right] = \frac{I_{Tot}-I_{RR}-I_M}{2\sqrt{I_{RR}I_M}} = g^{(1)}\left[(x,y),(-x,-y)\right]\sin\left(\omega\Delta t+\varphi_0\right)$ where I_{Tot} is the total intensity of the interference pattern, I_{RR} (I_M) is the intensity recorded from the arm with the retroreflector (single mirror), ω is the frequency of the periodic pattern of the interference fringes and φ_0 is the initial phase of the condensate. For each point of the condensate a sinusoidal evolution of the normalized interference as a function of the delay Δt is recorded. The first order coherence of each point of the condensate is extracted with the help of the previous formula; and repeating this procedure for each point we can reconstruct the entire coherence map.

At E_{Th}, the interference pattern extends along the entire condensate (Fig. 1(a)) and the corresponding coherence map (Fig. 1(b)) reveals that the phase is locked across the entire area, and a single coherent mode is formed, validating the theoretical predictions [12]. This is shown in detail in Fig. 1(c), which depicts the coherence of a horizontal profile ($0.26\,\mu$m width) taken at the center of the map. The fact that the degree of coherence is almost flat along the entire condensate demonstrates that only a single coherent mode is formed, in contrast with what has been found in previous works [20, 25] where disorder of the sample caused the development of several modes. The extension of the coherence here is $\sim 40\,\mu$m. Until now only Baas *et al.* [26] have obtained similar levels of extended spatial coherence in the OPO condensate, though without the complete quantitative map of $g^{(1)}$ presented here (the still longer coherence lengths, as already mentioned in the introduction, observed in 1D microcavities [4] are associated with polaritons propagating outside the pumped region). It is worth to note that in an OPO process, the coherence properties of the signal are not inherited from the excitation laser [27]. Although the theory of an infinite 2D condensate predicts the absence of long-range order, and a power-law decay of the spatial coherence [5] with a decay length inversely proportional to

#185756 - $15.00 USD Received 22 Feb 2013; revised 15 Apr 2013; accepted 17 Apr 2013; published 25 Apr 2013

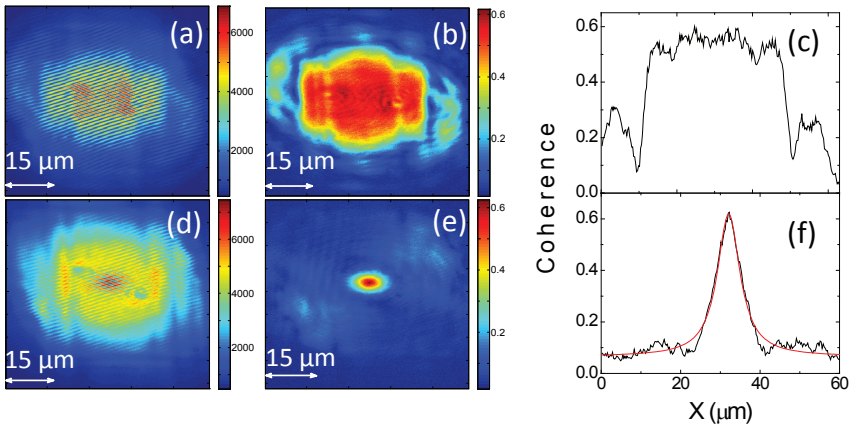

Fig. 1. Interference pattern (a/d) and corresponding coherence (b/e) of the condensate generated at/below the parametric threshold, E_{Th}, corresponding to a pump energy $E_1 =$ 1552.574 meV/ $E_2 = 1552.567$ meV and power density $P = 15.8\,\mathrm{kW/cm^2}$. Horizontal profiles at the center (c/f) showing the constant coherence along the entire condensate for E_1, and an exponentially decaying one for E_2.The red line is the Lorentzian fit.

the particles' mass, in a finite dimension system such as ours, determined by the pump laser size which is much smaller than the decay length, a constant coherence of the condensate can be obtained [3]. By decreasing the pump energy by $\delta E \equiv E_{Th} - E = 0.008$ meV towards lower energies, leaving fixed the pump angle, the phase matching conditions for the OPO are not fulfilled anymore and an emission of thermally populated states is obtained at the bottom of the LPB. The interferometric analysis of the emission from the cloud of non-condensed polaritons gives an interference pattern only at the center of the emission (Fig. 1(d)). The corresponding coherence map (Fig. 1(e)) reveals a $\sim 7\,\mu$m coherence length, extracted by fitting the profile of the spatial decay to a Lorentzian function (Fig. 1(f)). Repeating the measurements for different values of δE we recover the same coherence length of the order of $\sim 6\,\mu$m, as depicted in Fig. 2, which is limited by the cavity lifetime. These results demonstrate the predictions of Ref. [12] about the coherence of polariton emission below and at the condensation threshold. Measuring $g^{(1)}(\tau)$ at a given point for different time delays τ permits the evaluation of the signal temporal coherence $g^{(1)}(\tau) = \frac{\langle E^*(t)E(t+\tau)\rangle}{\langle E^*(t)\rangle\langle E(t)\rangle}$. In our case we obtain $g^{(1)}$ for different values of the condensate area A and pump power density P_d, as shown in Fig. 3. The variation in area is obtained changing the optics before the lens focusing on the sample, so that the range of pump angles does not change. In this way we are able to perform a controlled comparison with theory, by varying the area while maintaining the same power density. We obtain a predominantly exponential decay for $g^{(1)}(\tau)$, with a coherence time reaching $T_c = 3.2$ ns (see the definition of T_c below). This is six times longer than the largest value reported in the literature until now for the same material system [17]. Despite the lack of spatial fluctuations, the coherence time of our condensate, though long, is clearly finite. In general, such a finite correlation time in a state with perfect spatial order is caused by finite-size fluctuations [28], and reflects the absence of true phase transitions in finite systems. A well-known example is the Schawlow-Townes formula for the coherence time of a single laser mode with an average of $\bar{N}$ photons, $T_c \propto \bar{N}$. Since

#185756 - $15.00 USD Received 22 Feb 2013; revised 15 Apr 2013; accepted 17 Apr 2013; published 25 Apr 2013

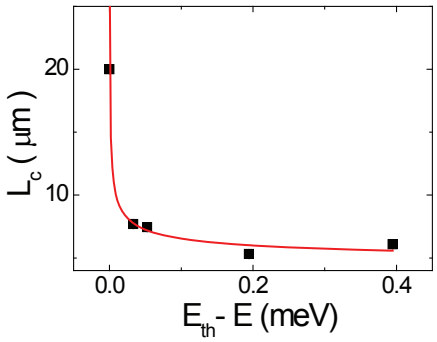

Fig. 2. Coherence length L_c as a function of the energy distance from the threshold $\delta E \equiv E_{Th} - E$. Red line is a guide to the eye.

$\bar{N} \propto A$ when the control parameter P_d is constant, the Schawlow-Townes result implies the scaling form $T_c \propto A$. However, as shown in detail below, this scaling law is violated by more than an order of magnitude for our condensate, and our results cannot be understood as a straightforward effect of increasing the particle number. Our results may be interpreted in terms of the theoretical model of Ref. [14], in which the linewidth arises from fluctuations in the number of particles. Due to the interactions, such number fluctuations imply energetic fluctuations of the emission, leading to a broadened line or a decay of $g^{(1)}(\tau)$. This is captured by Kubo's result

$$\left|g^{(1)}(\tau)\right| = \exp\left[-\frac{2\tau_r^2}{\tau_c^2}\left(e^{-\tau/\tau_r} + \frac{\tau}{\tau_r} - 1\right)\right], \tag{1}$$

for the emission from a transition whose energy fluctuates, where τ_c is determined by the width of the (generically Gaussian) distribution of the energy level and τ_r is the characteristic timescale on which the fluctuations occur. If $\tau_r \gg \tau_c$ the fluctuations are slow and the emission reflects the energy distribution of the level, so that the coherence decays on timescale τ_c. If however $\tau_r \ll \tau_c$ a motional narrowing effect leads to an exponential decay, with a much longer coherence time $T_c = \tau_c^2/2\tau_r$. To elucidate the effects of number fluctuations, we fit the data in Fig. 3 to the Kubo formula (1), the error bars of the fit parameters τ_r and τ_c are estimated from the regression to Eq. (1) and explicitly shown in Figs. 3(c) and 3(d). Pumping with the same power density P_d, defined as the ratio between the average power P_{ave} and the condensed area A_c ($P_d = P_{ave}/A_c$) $P_d = 10\,\mathrm{kW/cm^2}$, the condensate with a larger area $A = 2.7 \times 10^3 \mu\mathrm{m}^2$ presents $\tau_c = 0.97$ ns and $\tau_r = 0.15$ ns fulfilling the inequality for the motional narrowing regime and giving a coherence time $T_c = 3.2$ ns. For an intermediate area $A = 1.3 \times 10^3 \mu\mathrm{m}^2$ we observe a decrease of both parameters $\tau_c = 0.76$ ns and $\tau_r = 0.14$ ns corresponding to $T_c = 2.1$ ns, and reducing further the area to $A = 70\,\mu\mathrm{m}^2$, we obtain $\tau_c = 0.20$ ns and $\tau_r = 0.023$ ns corresponding to a shorter $T_c = 0.9$ ns, still indicating in both cases the system being in the motional narrowing regime. As well as moving to larger areas, another way to have longer decay times, suggested by [14], is to increase the pump power, with the pump always in the conditions to drive the system in the OPO regime. The results shown in Fig. 3(b), corresponding to two different powers keeping now the size of the condensate constant, also demonstrate that increasing the power a longer coherence time is achieved. In fact the coherence time for a condensate of relatively small area $A = 70\,\mu\mathrm{m}^2$ goes from $T_c = 0.5$ ns at $P_d = 5.4\,\mathrm{kW/cm^2}$, to $T_c = 0.9$ ns at $P_d = 10\,\mathrm{kW/cm^2}$. We note that the coherence decay of the smallest condensate at lowest power, black squares in Fig. 3(b), has considerable structure and does not follow the Kubo form, in fact neither a Gaussian nor exponential decay provides a good fit to this data, suggesting that this

#185756 - $15.00 USD Received 22 Feb 2013; revised 15 Apr 2013; accepted 17 Apr 2013; published 25 Apr 2013

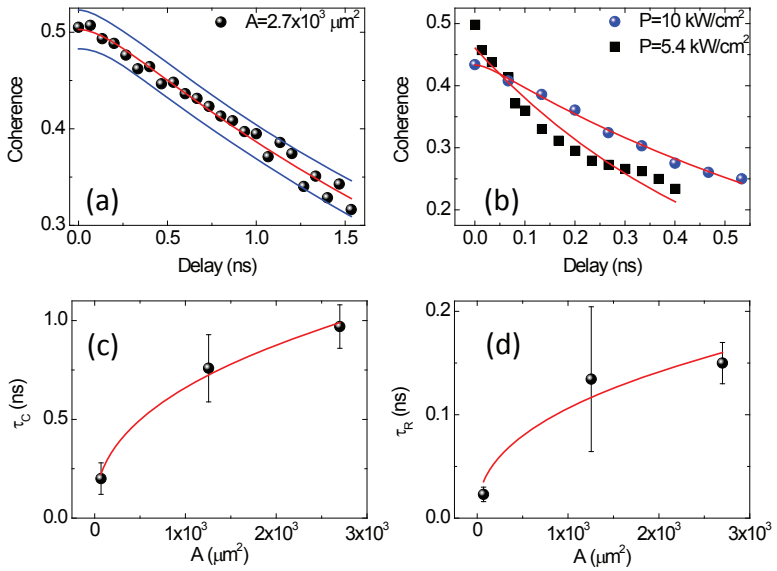

Fig. 3. (a) Temporal coherence decay above parametric threshold for condensate area $2.7\times10^3\,\mu\mathrm{m}^2$ at a pump power density $P_d = 10\,\mathrm{kW/cm}^2$, the central line is a fit to Eq. (1), side bands define the confidence range in which the experimental points fall within a probability of 95%. (b) Temporal coherence decay for $P_d = 5.4\,\mathrm{kW/cm}^2$ (black squares) and $10\mathrm{kW/cm}^2$ (blue dots) at $A = 70\,\mu\mathrm{m}^2$. Lines are fits to Eq. (1); (c) τ_c as a function of the condensate area A, the line is a fit to $\tau_c \propto A^x$, with $x = 0.41 \pm 0.05$; (d) τ_r as a function of condensate area A, the line is a fit to $\tau_r \propto A^x$ with $x = 0.41 \pm 0.17$.

condensate is not a single mode. It is worthwhile mentioning that to obtain condensates of different areas keeping the polariton density constant, we magnify the driving pump area by a known factor and we adjust the laser pump in order to achieve that the condensate areas scale by the required factor. Assuming that the power driving the condensates is proportional to the laser power, creating them at the same distance from the power threshold, and taking into account the changes in the acceptance angle for different condensate areas, this procedure assures that the density of polaritons in the condensates can be kept the same within an error of 20%. From the Kubo fits to our data, for a given power, we can extract the scaling $\tau_c \propto A^{0.41\pm0.05}$ (Fig. 3(c)). This is consistent with the dominant dephasing mechanism being the polariton-polariton interaction, suppressed by motional narrowing, in which case the Kubo formula should hold with $\tau_c \propto A^{0.5}$ [14]. Although this implies an increase in the coherence time, T_c, with area, our results show that this increase is restrained because τ_r also increases with area as $\tau_r \propto A^{0.41\pm0.17}$ (Fig. 3(d)), so that motional narrowing becomes less effective, giving to the coherence time the trend $T_c \propto A^{0.5}$. This is shown in Fig. 4 that depicts T_c as obtained from a fit to an expression similar to Eq. (1) which has been rewritten to explicitly contain T_c as a parameter,

$$\left|g^{(1)}(\tau)\right| = \exp\left[-\frac{\tau_r}{T_c}\left(e^{-\tau/\tau_r} + \frac{\tau}{\tau_r} - 1\right)\right]. \tag{2}$$

Note that the error bars of T_c are estimated from the regression to Eq. (2). The red solid line shows the best fit to a square root dependence on A, while the dashed line corresponds to a linear dependence (Schawlow-Townes mechanism). We note that the square root form provides a

#185756 - $15.00 USD Received 22 Feb 2013; revised 15 Apr 2013; accepted 17 Apr 2013; published 25 Apr 2013

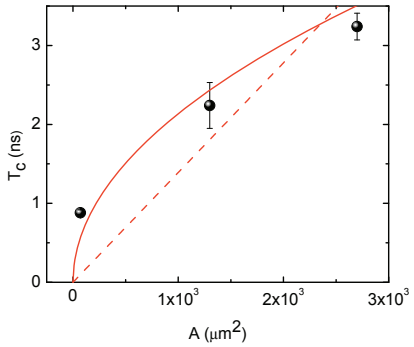

Fig. 4. Temporal coherence T_c as obtained from Eq. (2) as a function of the condensate area A. Red solid line is a fit to square root dependence on area A, dashed line corresponds to the best fit to a linear dependence.

better fit to the data, consistent with the linewidth due to polariton-polariton interactions in the motional narrowing regime. The relatively small size of our system and the use of pump powers which are close to threshold, P_{Th}, are responsible for the observed increase of τ_r with area. In the thermodynamic limit, $A \to \infty$, the occupation, n, of a single mode with linear gain γ, linear loss γ_c and nonlinear gain Γ obeys the mean-field rate equation $dn/dt = (\gamma - \gamma_c - \Gamma n)n$ [29]. Linearizing we see that the damping time for number fluctuations is $\tau_r = 1/|\gamma - \gamma_c|$. This timescale is therefore independent of area when the rate equation is valid. However, at power threshold, $\gamma = \gamma_c$ and the rate equation predicts a divergence in the relaxation time, which in the finite system must be cut off by fluctuations. Thus, in the threshold region, τ_r initially grows with area, as we observe, before eventually saturating. The scaling in the threshold region may be obtained from the dynamical model described in Ref. [14], which when solved numerically at threshold gives $\tau_r \propto \sqrt{A}$, consistent with Fig. 3(d). For completeness we also studied the temporal coherence (not shown) under two further conditions: a) Exciting the LPB at the inflection point, for power densities slightly above but very close to P_{Th}, we find a Gaussian decay of $g^{(1)}(\tau)$, as previously observed for condensates with non-resonant pumping [20]. This is consistent with the expected increase in τ_r approaching P_{Th} causing a crossover from the motional-narrowing to the static regime. b) Exciting far from the inflection point we observe a very fast exponential decay of coherence in the range of the polariton lifetime due to the fact that no condensation is achieved in this case.

4. Conclusions

In summary, we have investigated the spatial and temporal coherence properties of polariton condensates generated by parametric scattering. The spatial coherence was studied below and above the OPO condensation threshold, obtaining a very large coherence length for 2D GaAs microcavity polaritons. Measurements of the temporal coherence reveal a predominantly exponential decay caused by polariton-polariton interactions in a motional narrowing regime. Although similar to the exponential decay associated with the Schawlow-Townes linewidth, the mechanism is different, and gives a different dependence of coherence time on condensate area. By varying the area of the condensate and comparing with scaling laws, we observe that the dephasing time follows the predictions of the coherence theory of polariton condensates. Constructing condensates of large area, we are able to achieve long coherence times, which is a crucial step forward for exploiting polariton condensates in quantum and ultrafast devices.

#185756 - $15.00 USD Received 22 Feb 2013; revised 15 Apr 2013; accepted 17 Apr 2013; published 25 Apr 2013

Acknowledgments

The work was supported by the FP7 ITNs Clermont4 (235114) and Spin-optronics (237252), Spanish MEC (MAT2011-22997), CAM (S-2009/ESP-1503), and Science Foundation Ireland SIRG/I1592 (PRE). We thank C. Tejedor and I. Carusotto for valuable discussions.

#185756 - $15.00 USD Received 22 Feb 2013; revised 15 Apr 2013; accepted 17 Apr 2013; published 25 Apr 2013